IEEE/CSC & ESAS European Superconductivity News Forum (ESNF), No. 15, January 2010
Published in Supercond. Sci. Technol. (SuST) **23** (2010) 124002 (7pp)

Influence of post-growth thermal treatments on the critical current density of TSMG YBCO bulk superconductors

P. Diko[1], V. Antal[1], K. Zmorayová[1], M. Šefčiková[1], X. Chaud[2], J. Kováč[1], X. Yao[3], Chen X.[4] , M. Eisterer[5], H. W. Weber[5]

[1] Institute of Experimental Physics SAS, Watsonova 47, 04001 Košice, Slovakia

[2] CNRS/CRETA, 25, Avenue des Martyrs, 38042 Grenoble Cedex 9, France

[3]Department of Physics, Shanghai Jiao Tong University, 800 Dongchuan Road, Shanghai 200240, People's Republic of China

[4]Department of Materials Science and Engineering, National Cheng Kung University (NCKU) Tainan, Taiwan

[5] Vienna University of Technology, Atominstitut, Stadionallee 2, 1020 Vienna, Austria

Abstract. Oxygenation and thermochemical post-growth treatments of top seeded meltgrowth (TSMG) YBCO bulk superconductors can significantly influence critical current density. It is shown that, depending on oxygenation conditions and the size of 211 particles, different reductions of intrinsic critical current density values can be obtained due to the reduction in the sample

cross-section caused by the presence of *a/b*-microcracks induced by 211 particles, and *a/b*- and *a/c*-cracks induced by oxygenation. The possibility of eliminating oxygenation cracks by high pressure oxygenation and consequently significantly increasing the macroscopic critical

current density is demonstrated. An effective dopant concentration for chemical pinning is proposed and possible clustering of substitutions in the Y123 lattice by thermochemical treatments is shown.

1. Introduction

The problems related to weak links at high-angle grain boundaries and insufficient flux pinning in high temperature superconductors were solved in the case of $YBa_2Cu_3O_{7-x}$ (Y123 or 123)/Y_2BaCuO_5 (Y211 or 211) composite bulk superconductors by employing a so-called top seeded melt-growth (TSMG) process. The increased understanding of the growth mechanisms of the bulk melt-processed 123/211 composite superconductors has led to improvements in growth conditions with the goal of increasing trapped field and levitation force, particularly in high magnetic fields. These are the most significant properties that are important for practical applications and are influenced by crystal defects formed at different stages of bulk superconductor fabrication. They have positive (pinning centres) or negative (weak links) effect on critical current density. 211 particles and stresses around them, added nanoparticles, dislocations, stacking faults, point defects, substituted atoms (dopands) and twins can be considered as the most important pinning centres. Weak links are present in the form of subgrain boundaries, cracks and porosity. Parameters of the TSMG process mainly influence the macroscopic homogeneity of 211 particle distribution (dependence of 211 volume fraction on the distance from the seed) or the distribution of other added solid particles and consequently macroscopic thermal dilatation stresses and local twin spacing.

Processing parameters also influence the macroscopic distribution of dopands, as well as the formation of subgrains and pores in the bulk single-grain samples [1]. On the other hand, post-growth treatments may also significantly modify the quality and quantity of crystal defects in these bulks. In this paper we will consider mainly the influence of applied post-growth treatments on cracking as well as on possible changes in the rearrangement of dopant atoms in the Y123 crystal lattice and their relation to the critical current density.

2. Map of cracking caused by postgrowth treatment

When the microstructure of the TSMG YBCO single-grain samples is observed under a microscope after etching, three types of cracks can be found. The most typical are microcracks along *a/b*-planes (*a/b*-microcracks, *a/b*-MIC), traces of which can be seen on the *a/c*-surface as dense lines paralel to the *a/b*-planes. Their length does not exceed some 211 interparticle distances (figure 1(a)). It was shown in our previous studies [2] that the *a/b*-microcracks are formed in TSMG bulks due to thermal dilatation microstresses induced by 211 particles. It has also been shown that a critical 211 particle radius, R_{C211}, exists. 211 particles smaller than this critical size do not create enough elastic energy to form a crack. For 123/211 composite, R_{C211} was estimated to be 0.24 μm. The subcritical 211 particles, which are not able to nucleate any *a/b*-microcracks, can be seen in figure 1(b). 211 particles and *a/b*-microcracks can reduce the effective cross-section by up to 30% of its original value [3].

The oxygenation process of single-grain YBCO bulks is accompanied by the formation of another type of crack called an oxygenation crack [2] (figure 2). The oxygenation cracks are parallel to the cleavage planes of the 123 phase, which are the *a/b*- and *a/c*-planes ({100} and {001} planes). The reason for cracking is the shortening of the *c*-lattice parameter as well as the shortening of the average *(a + b)/*2 lattice parameter of the 123 phase with the oxygen content in the 123 phase, which induces tensile stresses in the oxygenated surface layer in the *c*-, *a*- and *b*-directions (<001> and <100> directions). At the critical thickness of the oxygenated layer, d_{cr},

$$d_{cr} = 0.5K_{IC}^2/(E\varepsilon)^2 \qquad (1)$$

(*E*—Young's modulus, K_{IC}—fracture toughness, ε—strain in the oxygenated layer) a regular pattern of cracks perpendicular to the acting tensile stress develops with the spacing, λ, proportional to the stress in the layer, and the thickness of the oxygenated layer, *d*, such that

$$\lambda = 5.6\{K_{IC}^2 d/(E\varepsilon)^2\}^{1/2} \qquad (2)$$

The developed oxygenation cracks are an important microstructural element of TSMG bulk superconductors because they influence technological, superconducting and mechanical properties of these materials. They significantly reduce the time necessary for full oxygenation of the bulk sample to one or two weeks. Without these cracks, the oxygenation process will be conducted only through oxygen bulk diffusion and at usual oxygenation temperatures of around 400 ˚C it will take thousands of years [4, 5]. The oxygenation cracks parallel to the *a/b*-plane do not influence the superconducting properties very much as they are parallel to the supercurrent. The oxygenation cracks parallel to the *a/c*-plane have a more serious influence on the superconducting properties as they reduce the effective cross-section of the sample. Simple analysis done by Eisterer [3] showed that the reduction of intrinsic critical current density, J_{c0}, for supercurrent flowing along the {001}- plane is proportional to the l/λ parameter

$$J_c = J_{c0}\{ 1 - 0.93\ (l/\lambda)^{1/2}\} \qquad (3)$$

where l is the mean crack length and λ is the crack spacing of the cracks perpendicular to the {001}-plane. Measurement of these parameters estimated $l/\lambda = 0.5$ [6]. This value points out
that the intrinsic critical current density should be about three times higher than the value estimated from magnetization or transport measurements. We tested the 123 single-crystal for the presence of oxygenation cracks. Microstructural analysis of a Nd123 single-crystal of size 1.5×1.5mm^2 in the *a/b*-plane and 1 mm in the *c*-direction, annealed at 340 ˚C for 200 h in oxygen gas flow, revealed oxygenated cracks with $l/\lambda = 0.53$ [7]. In these case the oxygenation cracks parallel to the *c*-direction were partially declined from the *a/c*-plane with maxima at 45◦ to the *a/c*-plane (figure 3). The question is how we may eliminate the formation of these oxygenation cracks and at the same time keep a short oxygenation time. The oxygen diffusion rate can be significantly increased at higher oxygenation temperature, and high enough equilibrium oxygen content in $YBa_2Cu_3O_{7-x}$ can be reached by higher oxygen pressure [8]. At the same time, the oxygen gap between the surface oxygenated layer

and the core tetragonal phase must be kept lower than the critical one for crack formation. Oxygenation at 750˚C and the pressure from 160 bars of small samples cut from the TSMG YBCO bulk confirmed the possibility of eliminating oxygenation cracks and the expected significant increasing of J_c [9, 10] (figure 4). As the critical oxygen gap is lower for *a/b*-crack formation than for *a/c*-crack formation and the *a/b*microcracking is influenced by the size of 211 particles, we may obtain six different cracking microstructures depending on the oxygenation parameters and the size of 211 particles with related reduced effective sample cross-section as expressed in figure 5. In the case of standard YBCO bulk superconductors, the measured critical density is about one order of magnitude lower than that for the crystal free of oxygenation cracks and *a/b*-microcracks. Besides high pressure oxygenation, further significant *J*c increase can be achieved by replacing 211 particles with other effective pinning centres, which do not nucleate *a/b*-microcracks [11].

3. Optimum dopant concentration for chemical pining

Pinning by substitution atoms (dopants) in the Y123 lattice (also called chemical pinning) has been studied in TSMG YBCO bulks and it was shown that it can improve critical current density at medium magnetic fields and improve trapped field [12–15]. It is supposed that the regions with suppressed superconductivity around single atoms are effective pinning centres. The size of these regions with suppressed superconductivity due to stress field or locally induced magnetic moment is about 1.5–2 nm [16, 17]. These pinning centres are smaller than the diameter of the magnetic flux line (FL), which is about 6 nm at 77 K (two coherence lengths). An effective dopant concentration for pinning should exist and can be estimated from the consideration expressed in figure 6. Bending of the flux line to fit to the position with the lowest energy in the randomly distributed field of point pinning centres with mean distance $\lambda_{PC} \geq 2\xi$ and size $d < \xi$ leads to pinning. On the other hand, the position of the flux line in the field of dense ($\lambda_{PC} << 2\xi$) randomly distributed chemical pinning centres does not lead to energy saving and consequently the flux line is not pinned. Then, for the substitution in CuO chains, the mean distance of substituted atoms M in the CuO-plane, (λM), would be

$$\lambda_M = a/(x_M)^{1/2} \qquad (4)$$

where x_M is the dopant concentration expressed as $YB_2Cu_{1-x}M_xCu_2O_7$ and a is the Y123 lattice parameter (a = 0.38 nm). For λ_M = 6 nm we obtain $\boldsymbol{x}_M$ = 0.004. For YBCO stoichiometry expressed as $YB_2(Cu_{1-x}M_x)_3O_{7-x}$, $x = \boldsymbol{x}_{M/3}$ = 0.0013. At this concentration all CuO layers will be occupied by dopant atoms and the spacing of these layers in the *c*-direction would be 1.2 nm. The optimum mean distance of dopants in the *c*-direction should be related to the possible curvature of the bent FL, therefore we may suppose that the optimum dopant concentration will be even lower than $x_{M/3}$ = 0.0013. Consideration for the substitutions in the CuO_2 planes will lead to similar optimum dopant concentrations.

Referred nominal concentrations for chemical pinning in YBCO TSMG bulks are much higher than the optimum concentration $\boldsymbol{x}_{M/3}$ = 0.0013 (x_{Zn} = 0.004 [13], x_{Li} = 0.006 [18], x_{Ag} = 0.05 [19], x_{Al} = 0.0025 and 0.05 [10]). This higher nominal concentration can be caused by clustering of dopant atoms, by macroscopic inhomogeneity of dopant distribution in YBCO TSMG bulk developed during solidification or by parallel doping in the Y211 phase.

The observed influence of thermochemical treatment on effective Al concentration in Al doped YBCO bulks [10] can be caused by clustering of Al atoms. In figure 7 the various for SO (figure 8(a)) and at the highest concentration of Al (x = 0.05) for preannealing in argon (figure 8(b)). The peak effect, which we observed at the lowest Al concentrations, also confirms that the Al substitution in the Y123 lattice is close to the optimum concentration. Additional heat treatment of the samples with Al doping in argon at 800 ˚C for 2 h, followed by standard oxygenation, also caused significant changes in T_c. In the concentration range for x from 0.0025 to 0.02 we observed recovery of the transition temperature to the values found for the sample without Al substitution (figure 9). The distance between the disturbed regions, where T_c might be locally suppressed, increases by clustering of the Al atoms and T_c retains its original value in between. Thus, the Al doped samples behave as the undoped reference samples.

The second reason for high nominal dopant concentration in chemical pinning is that the real dopant concentration in Y123 solid phase, C_{MS0}, can be significantly lower than nominal, C_{M0}, due to the partition coefficient of the dopant between the solid and liquid phase kM = C_{MS0}/C_{M0}. As an example results on Ag doped Y123 can be illustrated. The observed dependence of the peak effect of the measured critical current density on the applied magnetic field at 77 K for the sample YBCO TSMG bulk with nominal composition $YBa_2(Cu_{0.95}Ag_{0.5})_3O_{7-x}$ (figure 10) suggests that the Ag concentration in the measured samples is much lower than nominal. According to wave dispersive microanalysis (WDS) measurements, the real Ag concentration in the measured sample is 0.12 at.% [19], which corresponds to the x = 0.005 in the $YBa_2(Cu_{1-x}Ag_x)_3O_{7-x}$ phase, but this is still about four times higher than the optimum dopant concentration x = 0.0013. If we suppose that Ag atoms are clustered with four atoms in one cluster, the distance between clusters would be close to the optimal one. The valence state of the Ag ion in the Y123 is considered to be monovalent with CN = 2 [22]. However, the unfavourable configuration (d) is always present when Ag substitutes Cu in the chains, as shown in figure 7(g). The concentration of this configuration can be minimized by one or two-dimensional clustering of Ag atoms (figures 7(h) and (i)). The two-dimensional square clusters with four atoms can fit well with the observed behaviour. Ag atoms can cluster during cooling to the temperatures where both the mobility of Ag ions in the Y123 lattice and the oxygen diffusion into the bulk are high enough. The temperatures higher than about 700 ˚C would be suitable for this process. The increasing of oxygen equilibrium concentration during the TSMG bulk cooling in air and the consequent increasing of Cu with the CN = 4 in the chains is then the reason for Ag clustering. It is an opposite process to the case of trivalent dopants where the low oxygen concentration leads to their clustering.

4. Conclusions

Formation of crystal defects during oxygenation and thermochemical heat treatments is an important phenomena in TSMG YBCO bulk superconductors. These post-growth treatments can influence the presence of weak links and modify the effectiveness of pinning centres. We have shown that, depending on oxygenation conditions and the size of 211 particles, different reductions of intrinsic critical current density values can be obtained due to the reduction in the sample cross-section caused by the presence of *a/b*-microcracks induced by 211 particles and *a/b*- and *a/c*-cracks induced by oxygenation. Elimination of oxygenation cracks by high pressure oxygenation and the consequent up to three times increased macroscopic critical current density is demonstrated. An effective dopant concentration for chemical pinning is proposed and possible clustering of substitutions in the Y123 lattice by thermochemical treatments is shown.

Acknowledgment

This work was realized within the frame of the projects „Centre of Excellence of Advanced Materials with Nano- and Submicron Structure (ITMS 262200120019), New Materials and Technologies for Energetics (ITMS26220220061), Research and Development of Second Generation YBCO Bulk Superconductors (ITMS26220220041), which are supported by the Operational Program “Research and Development” financed through European Regional Development Fund by VEGA project No.- 2/0211/10, Project ERANET- ESO and by the Centre of Excellence of Slovak Academy of Sciences NANOSMART.

References

[1] Diko P 2000 *Supercond. Sci. Technol.* **13** 1202

[2] Diko P 2004 *Supercond. Sci. Technol.* **17** R45

[3] Eisterer M *et al* 2006 *Supercond. Sci. Technol.* **19** S530

[4] Diko P, Granados X, Bozzo B and Kul´ık P 2007 *IEEE Trans. Appl. Supercond.* **17** 2961

[5] Diko P, Kaňnuchová M, Chaud X, Odier P, Granados X and Obradors X 2008 *J. Phys.: Conf. Ser.* **97** 012160

[6] Zmorayova K, Diko P and Krabbes G 2006 *Physica* C **445** 436

[7] Diko P, Zmorayová K, Šefčiková M, Antal V, Kováč J andYao X, 2010 unpublished

[8] Chaud X, Prikhna T, Savchuk Y, Joulain A, Haanappel E, Diko P, Porcar L and Soliman M 2008 *J. Phys.: Conf. Ser.* **97** 012043

[9] Diko P, Chaud X, Antal V, Kaňuchová M, Šefčiková M and Kováč J 2008 *Supercond. Sci. Technol.* **21** 115008

[10] Antal V, Kaňuchová M, Šefčıková M, Kováč J, Diko P, Eisterer M, H¨orhager N, Zehetmayer M, Weber H W and Chaud X 2009 *Supercond. Sci. Technol.* **22** 105001

[11] Hari Babu N, Iida K and Cardwell D A 2007 *Supercond. Sci. Technol.* **20** S141

[12] Krabbes G, Fuchs G, Schätzle P, Gruß S, Park J W, Gardinghaus F, Stöver G, Hayn R, Drechsler S-L and Fahr T 2000 *Physica* C **330** 181

[13] Shlyk L, Krabbes G, Fuchs G, Stover G and Nenkov K 2002 *Physica* C **377** 437

[14] Zhou Y X, Scruggs S and Salama K 2006 *Supercond. Sci. Technol.* **19** S556

[15] Ishii Y, Shimoyama J, Tazaki Y, Nakashima T, Horii S and Kishio K 2006 *Appl. Phys. Lett.* **89** 202514

[16] Fuchs G, Krabbes G, Müller K H, Verges P, Schultz L, Gonzalez-Arrabal R, Eisterer M and Weber H W 2003 *J. Low Temp. Phys.* **133** 159

[17] Pan S H, Hudson E W, Gupta A K, Ng K-W, Eisaki H, Uchida S and Davis J C 2000 *Phys. Rev. Lett.* **85** 1536

[18] Shlyk L, Krabbes G, Fuchs G, Nenkov K and Verges P 2003 *Physica* C **392** 540

[19] Diko P, Antal V, Kaňuchová M, Jirsa M and Jurek K 2010 *Physica* C **470** 155

[20] Takayama-Muromachi E 1990 *Physica* C **172** 199

[21] Renevier H P, Hodeau J L, Marezio M and Santoro A 1994 *Physica* C **220** 143

[22] Shannon R D 1976 *Acta Crystallogr.* A **32** 751

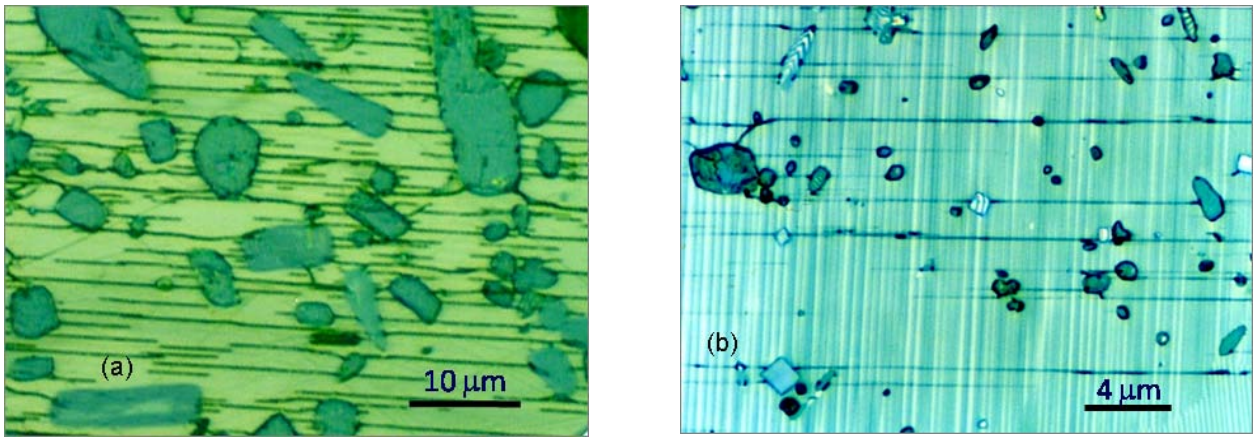

Figure 1. (a) Traces of *a/b*-microcracks seen on a polished and etched *a/c*-surface. (b) The 211 particles smaller than 0.5 µm do not nucleate *a/b*-microcracks.

.

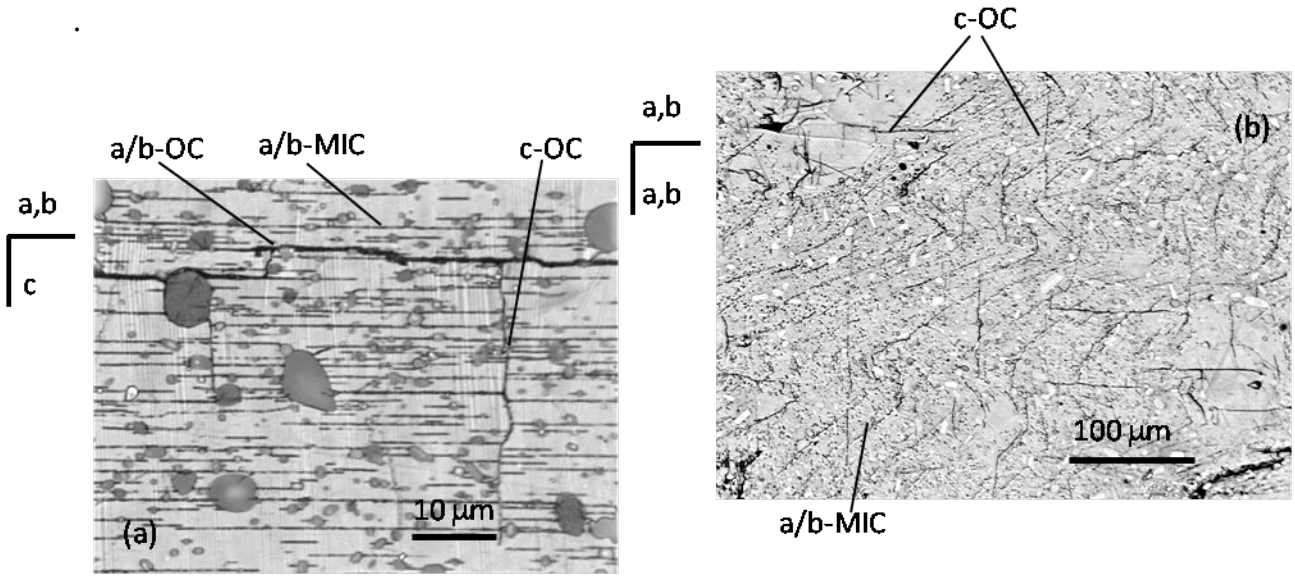

Figure 2. Traces of oxygenation cracks seen on polished and etched *a/c*- and *a/b*-surfaces. (a) Oxygenation cracks parallel to the *c*-direction (*c*-OC) start from the oxygenation cracks parallel to the *a/b*-plane (*a/b*-OC). (b) Traces of *c*-OC on the *a/b*-surface are perpendicular

and parallel to the *a/c*-crystal planes; traces of *a/b*-microcracks (*a/b*-MIC) are also seen due to crystal misalignments caused by subgrains.

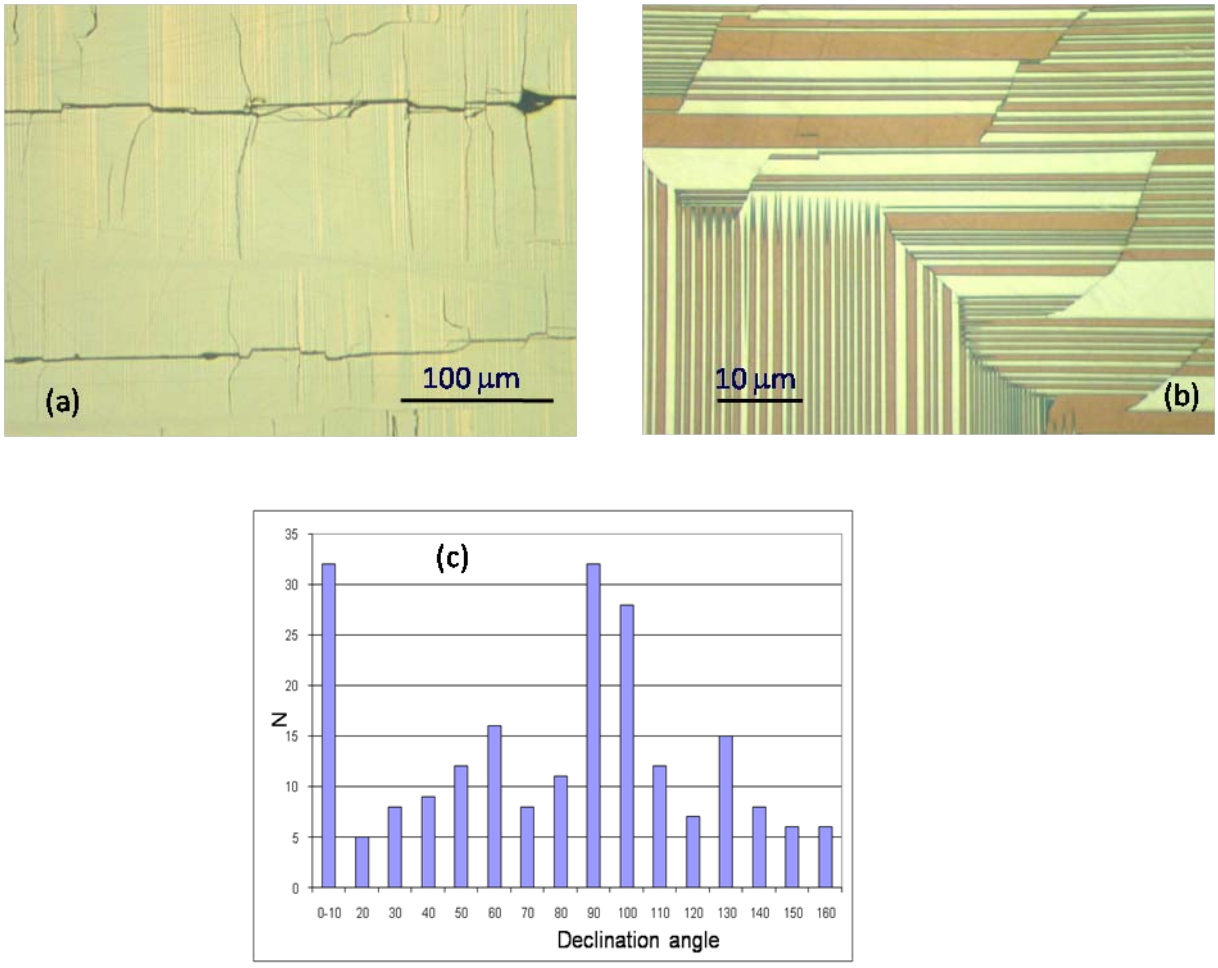

Figure 3. Oxygenation cracks developed in Nd123 single-crystal. (a) The polished and etched *a/c*-surface; *c*-oxygenation cracks start at the surface of *a/b*-oxygenation cracks. (b) The polished *a/b* surface; *c*-oxygenation cracks make discontinuities in the twin pattern. (c) The orientation of *c*-oxygenation cracks at the *a/b* surface expressed by the dependence between crack declination angle from the *a/c*-plane and its frequency, *N*.

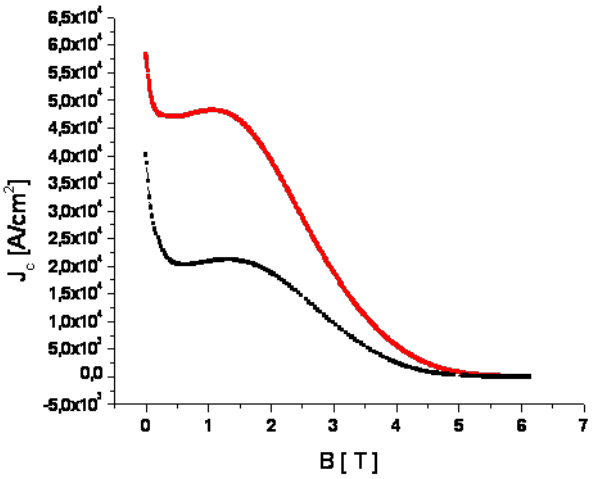

Figure 4. The critical current density at 77 K in the BSS sample $YBa_2(Cu_{1-x}Ag_x)O_7$ (x = 0.005) which is higher after high pressure oxygenation than after standard oxygenation [9].

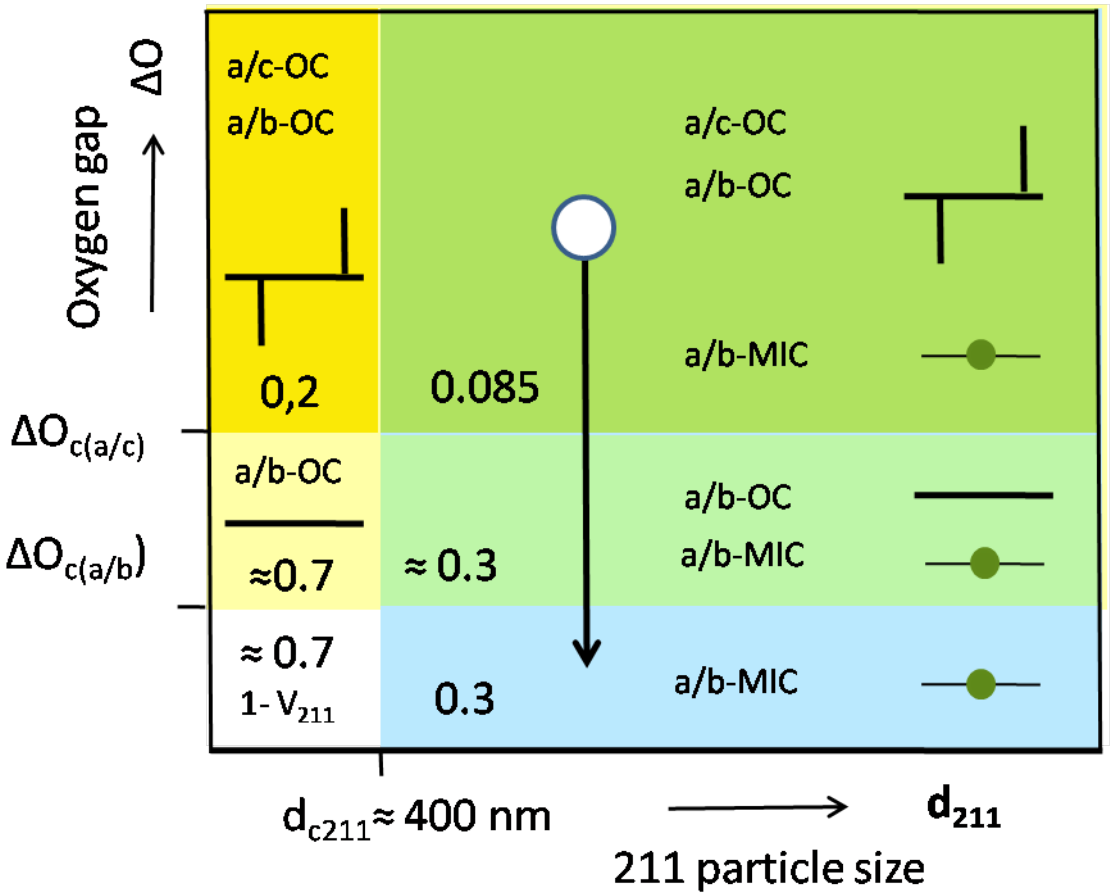

Figure 5. Schematic map of cracking for TSMG bulks. Six different fields with different crack combinations can be recognized depending on the oxygen gap (difference between oxygen concentration in the surface oxygenated layer and concentration in the core of the sample) and 211 particle size. $\Delta_{Oc(a/b)}$ and $\Delta_{Oc(a/c)}$ mean the critical oxygen gaps for the *a/b*-oxygenation crack (*a/b*-OC) and *a/c*-oxygenation crack (*a/c*-OC) formation. d_{c211} means the critical 211 particle size for *a/b* microcrack (*a/b*-MIC) formation. The number in each field expresses the reduction of the sample superconducting cross-section. The position of the standard YBCO TSMG samples is represented by a white circle, and a possible shift by elimination of oxygenation cracks is expressed by the arrow.

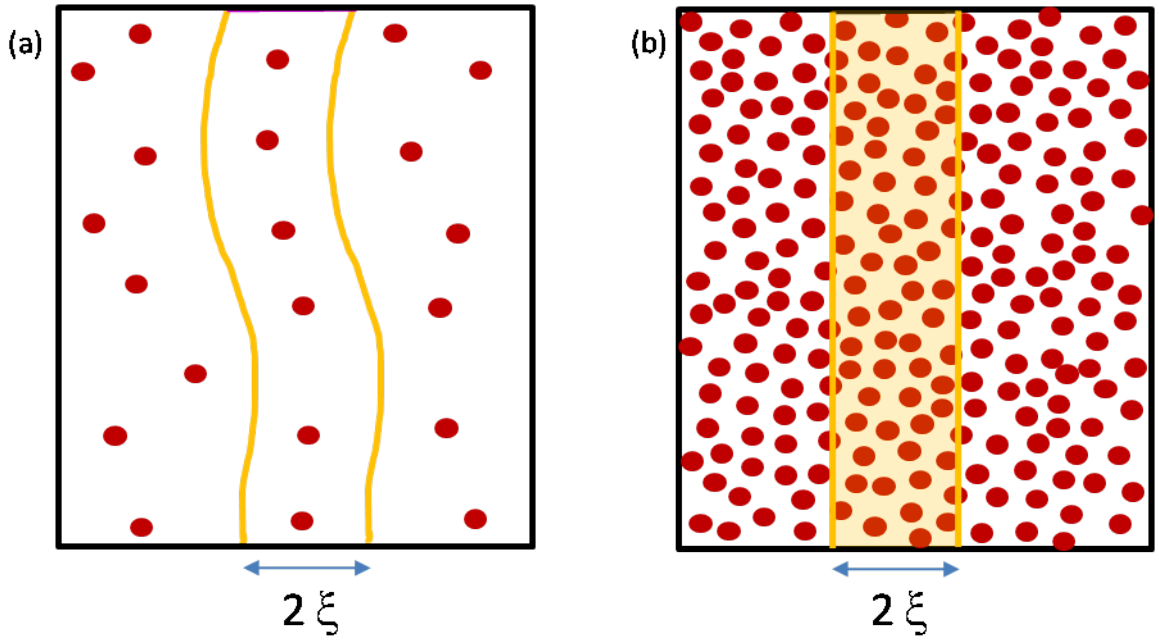

Figure 6. (a) Bending of the flux line to fit to the position with the lowest energy in the randomly distributed field of point pinning centres with mean distance $\lambda_{PC} \geq 2\xi$ and size $d < \xi$ leads to pinning. (b) A straight flux line in the field of randomly distributed pinning centres with mean distance $\lambda_{PC} << 2\xi$. The position of the flux line does not lead to energy saving and consequently the flux line is not pinned.

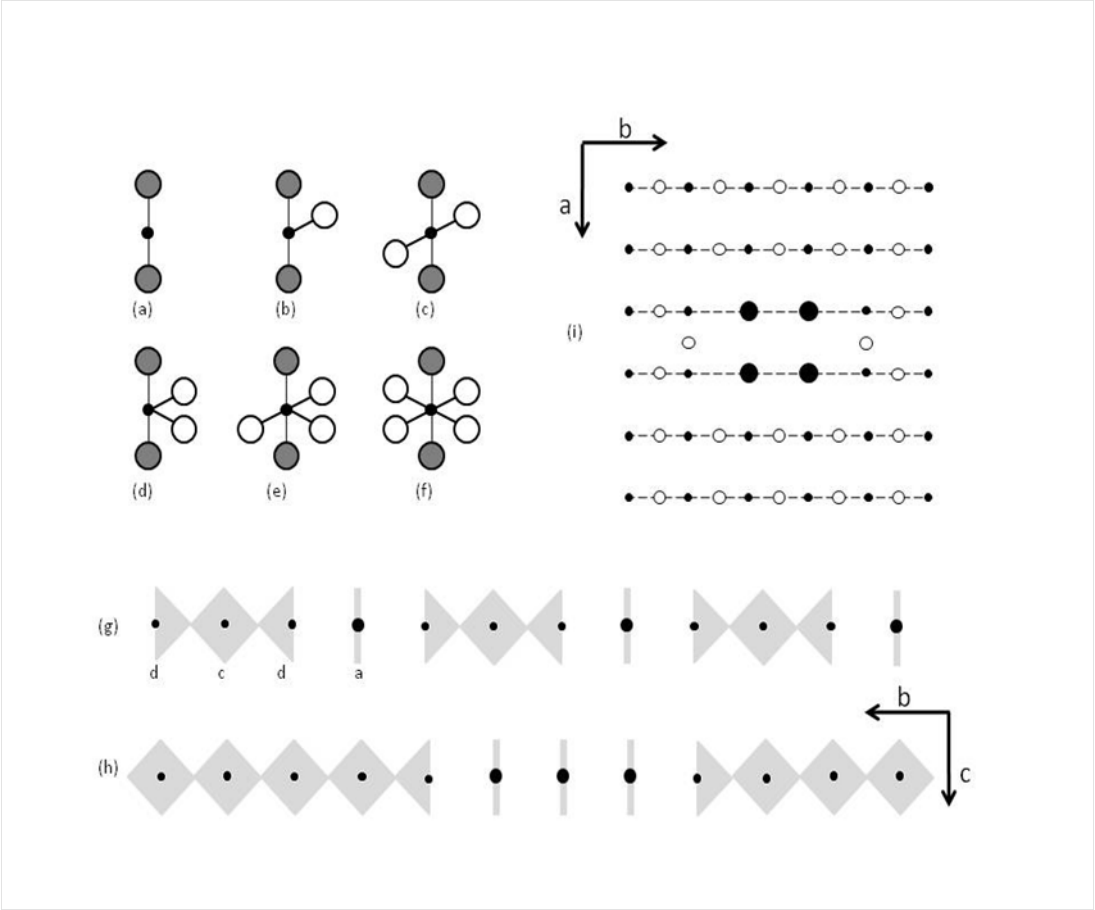

Figure 7. ((a)–(f)) Various oxygen configurations about the metal atom in the chains of the CuO-plane. The solid circle indicates the metal atom. The open and full circles indicate in-plane and out-of-plane oxygen atoms, respectively. ((g)–(i)) The concentration of (d) configurations is lower when linear (h) or two-dimensional (i) M clusters are formed. The smaller solid circles represent the Cu atoms and the larger ones represent the M atoms.

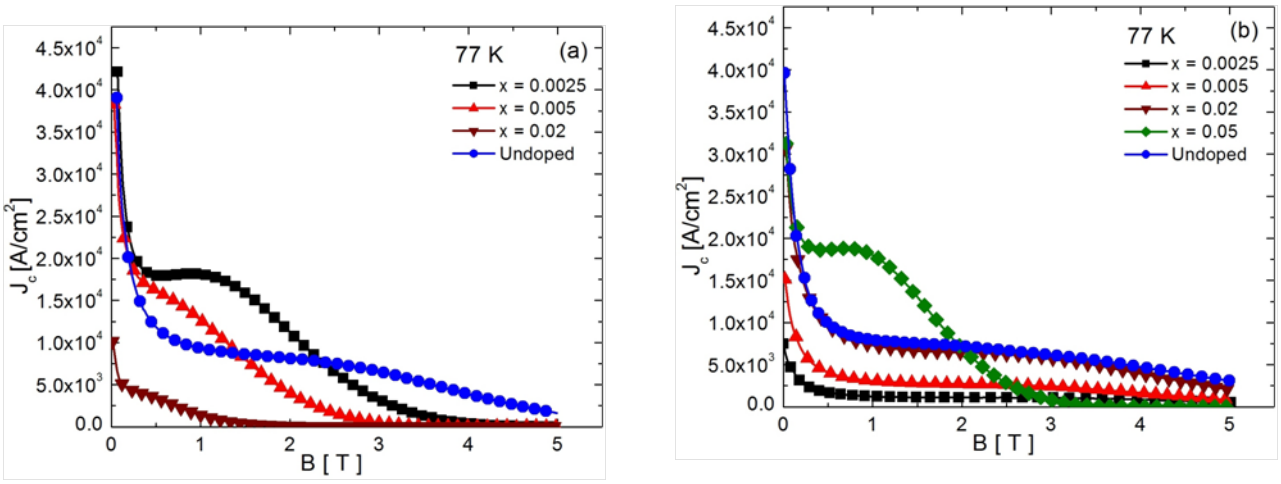

Figure 8. Dependence of the critical current densities, J_c, on magnetic field, B, at 77 K for $YBa2(Cu_{1-x}Al_x)_3O_{7-x}$ after standard oxygenation at 400 ˚C (SO) (a) and preannealing in argon at 800 ˚C (b).

.

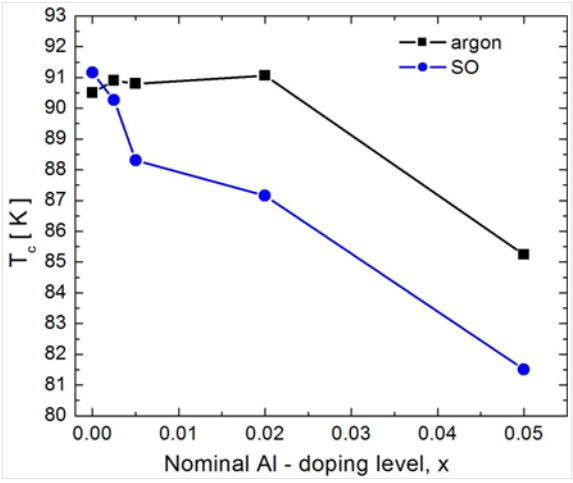

Figure 9. Transition temperature versus Al concentration for SO (circles) and preannealing in argon (squares).

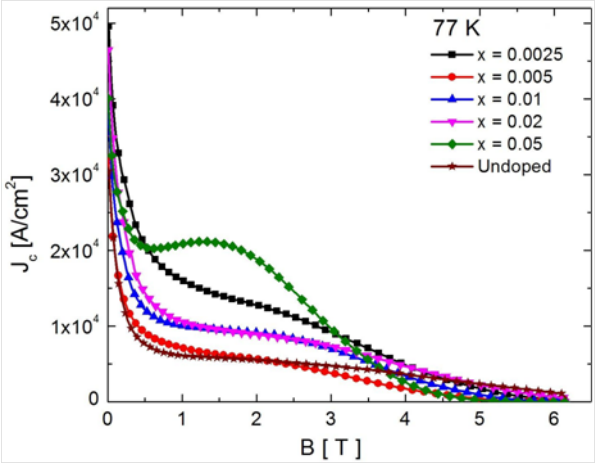

Figure 10. Dependence of critical current densities, J_c, on applied magnetic field, B, at 77 K for $YBa_2(Cu_{1-x}Ag_x)_3O_{7-\delta}$ after standard oxygenation.

.